University of Sistan and Baluchestan

Challenges in Nano and Micro Scale Science and Technology

Online ISSN: 2821 - 000X

Hydrothermal Synthesis of Nanostructure Mayenite Calcium Aluminate and Forming as a Support of Catalyst

Fatemeh Hooshyar[1] | Seyyed Hossein Zohdi[1]✉ | Abdolreza Samimi[1] | Ali Akbar Mirzaei[2]

1 Department of Chemical Engineering, Faculty of engineering, University of Sistan and Baluchestan, Zahedan, Iran
2 Department of Chemistry, Faculty of Sciences, University of Sistan and Baluchestan, Zahedan, Iran
Corresponding author's Email: zohdi@eng.usb.ac.ir

Article Info

Article type:
Research Article

Article history:
Received: 10 May 2026
Received in revised form: 09 June 2026
Accepted: 15 June 2026

Keywords:
Mayenite (C12A7),
Nanostructured,
In situ porosity generation,
Catalyst support

ABSTRACT

Mayenite ($Ca_{12}Al_{14}O_{33}$, C12A7) is a promising catalyst support due to its unique structural and electronic properties. However, conventional synthesis routes yield a low specific surface area, limiting access to active sites and reducing catalytic efficiency. In this work, we synthesized nanostructured mayenite via a hydrothermal method and subsequently shaped it into porous tablets using polyvinyl alcohol (10 wt%) and graphite (1 wt%) as pore formers, followed by pressing and calcination at 600 °C. The hydrothermally prepared powder initially showed a surface area of only 6.72 m^2/g. After the shaping and calcination process, the surface area increased to approximately 22 m^2/g, as confirmed by XRD, BET, and FESEM. Unlike conventional approaches, where sintering during forming reduces surface area, our method relies on in-situ porosity generation during the shaping step. This integrated approach provides a practical, scalable route to produce nanostructured, porous mayenite suitable for high-temperature catalytic applications such as Fischer–Tropsch synthesis.

INTRODUCTION

Mayenite, also known as C12A7 or $12CaO{\cdot}7Al_2O_3$, is a calcium aluminate compound that has attracted considerable interest in heterogeneous catalysis [1,2]. This material possesses a unique nanoporous crystalline structure composed of a positively charged framework, $[Ca_{24}Al_{28}O_{64}]^{4+}$, which encloses sub-nanometer-sized cavities [3,4]. Within these cages, an exchangeable anionic sublattice (X^-) can host various species, including O^{2-}, O^-, O_2^-, OH^-, and even electrons (e^-) [1,2]. A key consequence of this structural flexibility is the ability to trap and stabilize reactive oxygen species, which has positioned mayenite as a material of great significance in catalysis, particularly for oxidation reactions [5–7].

Owing to these unique structural and electronic properties, mayenite offers several advantages as a catalyst support. Its cage-like architecture promotes strong metal–support interactions and can significantly influence catalytic behavior [8,9]. Furthermore, mayenite exhibits excellent thermal stability, making it suitable for high-temperature reactions such as methane oxidation, where it has demonstrated enhanced activity compared to conventional supports [8,10]. Beyond oxidation, mayenite-supported catalysts have shown promise in hydrogenation, dehydrogenation, and other transformations [11]. The material's inherent resistance to carbon deposition and sulfur poisoning further broadens its potential applications, ranging from the oxidative destruction of hydrocarbons to serving as a non-noble metal catalyst or support [7,12,13].

Despite these advantages, conventional mayenite suffers from a low specific surface area (SSA), which reduces the available contact area for reactant molecules. Traditional high-temperature solid-state synthesis typically produces dense, sintered materials with an SSA rarely exceeding 1–5 m^2/g [10,14,15]. In heterogeneous catalysis, where reactions occur at the solid–gas interface, a low SSA severely restricts the concentration of accessible active sites and impedes reactant and product transport, thereby reducing catalytic efficiency [16]. Consequently, a major research goal has been to develop synthesis routes that yield high-SSA mayenite, unlocking its full catalytic potential.

Recent progress indicates that nanostructuring is essential for improving textural properties, and several innovative approaches have emerged as alternatives to conventional ceramic routes. For instance, Li et al. reported a hydrothermal method that produced mayenite

How to Cite this paper: Hooshyar F. Zohdi S.H. Samimi A. Mirzaei A.A. Hydrothermal Synthesis of Nanostructure Mayenite Calcium Aluminate and Forming as a Support of Catalyst. *Challenges in Nano and Micro Scale Science and Technology*. 2026; 14(1): 35-38. DOI: 10.22111/cnmst.2026.55319.1304

 Publisher: University of Sistan and Baluchestan.
DOI: 10.22111/cnmst.2026.55319.1304

with enhanced surface area, although subsequent ball-milling was often required [17]. Shuva Rakova et al. further streamlined this method by reacting CaO with an aluminum hydroxide suspension in water, yielding nanocrystalline mayenite with an SSA of approximately 80 m²/g after calcination at 600 °C [18]. Similarly, sol–gel methods using citrate or oxalate precursors have been used to produce nanocrystalline powders [19,20].

Another interesting route was developed by Meza-Trujillo et al., who employed solution combustion synthesis (SCS) with a dual-fuel system (urea/β-alanine) and oxalic acid as a pore generator. This method produced mesoporous mayenite with an SSA of 74 m²/g after calcination at 400 °C [21]. Using a modified glycine/nitrate method, Matovič and coworkers also obtained single-phase mayenite, illustrating the versatility of combustion routes [22]. A stepwise solid-state synthesis was patented by Qiao et al., in which pyrolysis and gasification of an organic pore-enlarging agent (e.g., starch or asphalt) create a micro-mesoporous structure, increasing the SSA to over 120 m²/g [23].

The work of Ruszak and colleagues shed light on the role of intermediate calcium aluminate phases (e.g., $Ca_5Al_6O_{14}$ and $Ca_3Al_2O_6$) that appear during the solid-state reaction starting from $CaCO_3$ and γ-Al_2O_3. They identified $Ca_5Al_6O_{14}$ as a key low-temperature intermediate—knowledge that can guide the design of energy-efficient calcination protocols while still yielding pure mayenite [24].

That said, the most effective methods for achieving high surface areas, such as aerogel synthesis with supercritical drying, are inherently complex, expensive, and difficult to scale for industrial use. The need for specialized equipment and precise control of supercritical conditions presents a major practical hurdle. Moreover, aerogel-derived samples remained largely X-ray amorphous even after calcination at 500 °C, crystallizing into a mixture of phases only at 900 °C, at which point the SSA collapsed to just 15–20 m²/g. Similarly, Meza-Trujillo et al. (2019) reported that their best high-SSA material (74 m²/g at 400 °C) still contained residual calcium carbonate. Upon obtaining pure crystalline mayenite at 800 °C, the SSA dropped significantly to 30 m²/g. This trade-off between crystallinity and porosity remains a fundamental challenge in materials science.

Therefore, in this work, we focus on the synthesis of mayenite nanoparticles by creating pores in situ during catalyst formation. A significant increase in SSA was achieved directly from the industrial forming process and subsequent binder removal, transforming a key limitation of the material into a functional advantage. We aim to realize a substantially enhanced surface area through particle size reduction to the nanometer range, thereby improving the performance of mayenite as an effective catalytic support.

Experimental

Synthesis of C12A7 Powder

Nanocrystalline mayenite ($12CaO{\cdot}7Al_2O_3$, C12A7) was synthesized via a hydrothermal method [13,17,25]. First, a stoichiometric mixture of $Ca(OH)_2$ and $Al(OH)_3$ (Ca:Al molar ratio of 12:14) was mixed for 4 hours. The resulting slurry was transferred to a Teflon-lined stainless steel autoclave for hydrothermal treatment at 150 °C for 5 hours. The solid product was collected, dried overnight at 120 °C, and subsequently calcined in static air at 1000 °C for 5 hours.

Shaping of C12A7 Powder into Porous Tablets

The synthesized C12A7 powder was formed into mechanically stable tablets for use as a catalyst support. First, the powder was sieved through a #50 mesh sieve. Then, a 10 wt% polyvinyl alcohol (PVA) solution was added dropwise with a syringe, followed by 1 wt% graphite as a secondary binder. The mixture was blended until it formed a smooth paste, which was then left at room temperature for 72 hours to partially dry. After that, the mixture was sieved through a #40 mesh sieve, yielding a granulated material with a weight loss of approximately 12%. The granules were pressed into tablets under uniaxial pressure. The tablets were dried at 120 °C for 4 hours to remove residual water and then calcined at 600 °C for 16 hours in air to ensure complete removal of the PVA binder. These conditions were determined from pre-experiments and thermogravimetric analysis to ensure complete oxidative removal of the PVA binder without sintering the mayenite framework. Figure 1 presents a schematic of the tablet support preparation.

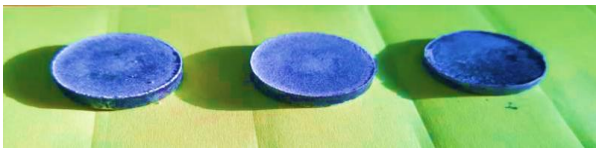

Fig. 1. Schematic of the tablet support preparation.

RESULTS AND DISCUSSION

Catalyst Characterization

X-ray diffraction (XRD) analysis was performed to identify the crystalline phases present using a Bruker D8 Advance diffractometer with Cu Kα radiation (40 kV, 30 mA). Figure 2 shows the XRD patterns of mayenite before and after tableting. For the mayenite (C12A7), characteristic peaks appeared at 2θ = 18.12°, 27.82°, 29.77°, 33.40°, 36.69°, 41.20°, 46.66°, 52.88°, 55.22°, 57.51°, 60.81°, 67.14°, and 72.22°.

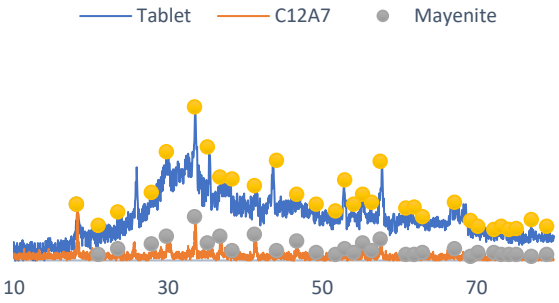

Fig. 2. X-ray diffraction (XRD) patterns of mayenite (C12A7) and tablet-formed mayenite (C12A7).

Surface area and porosity were evaluated via the BET method using a Quantachrome NOVA 2200 analyzer. To ensure accurate measurements, catalyst samples were degassed at 300 °C under N_2 flow for 3 hours prior to analysis to remove any physisorbed water or gases. Table 1 presents the BET and BJH analysis results for the C12A7 powder and porous C12A7 tablets. The BET surface area and pore volume increased from 6.72 m²/g and 0.03 cm³/g for the C12A7 powder to 21.73 m²/g and 0.09 cm³/g for the C12A7 tablets.

The use of high temperature (1000°C) for calcination of the synthesized powder was necessary, which led to a reduction in surface area compared to before calcination. However, the clever trick in the tablet preparation, while binding the particles together, leads to the release of gases resulting from the calcination of some of these organic compounds, and as a result, the porosity increases from 6.72 to 21.73 m^2/g

Table 1
BET results of structural properties of C12A7.

Sample	Specific Surface area ($m^2\ g^{-1}$) BET	Pore volume ($cm^3\ g^{-1}$)	Cumulative surface area ($m^2\ g^{-1}$) BJH
C12A7 powder	6.72	0.03	07.29
tablets C12A7	21.73	0.09	21.64

Figure 3 shows a field emission scanning electron microscopy (FESEM) image (at 80,000× magnification). The FESEM image of the products predominantly shows nanosheets along with nanoparticle crystals. The particles or structural features range in size from approximately 15 nm to 45 nm.

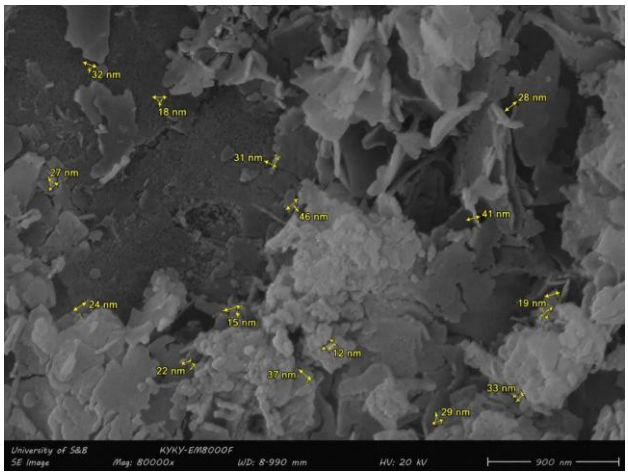

Fig. 3. FESEM image of tablet-formed mayenite.

CONCLUSIONS

In this work, by generating *in situ* pores during catalyst shaping, a significant increase in SSA was achieved directly from the industrial shaping process and subsequent binder removal. Although the initial hydrothermally synthesized mayenite powder exhibited a low SSA (6.72 m²/g)—typical for materials calcined at high temperatures—the shaping process itself was deliberately designed to create porosity. The addition of polyvinyl alcohol (PVA, 10 wt%) and graphite (1 wt%) as pore formers and binders, followed by their thermal removal during calcination at 600 °C, acts as a sacrificial templating step. During calcination, the PVA decomposes and combusts; its volumetric removal leaves behind a network of interconnected pores and voids within the pressed tablet structure. Concurrently, the graphite particles oxidize to CO_2. Furthermore, the nanocrystalline nature of the mayenite, with primary particles in the tens of nanometers range, further contributes to the development of a textured, porous architecture.

This process led to more than a threefold increase in SSA (from 6.72 to 21.73 m²/g). This gain is critically important for catalysis, as it directly increases the number of available surface sites for subsequent active phase deposition and reactant adsorption. The method efficiently combines material synthesis and catalyst shaping into a cohesive process. The shaping step is not merely for forming a mechanically stable pellet; rather, it is an active, functional step in tailoring the final catalyst's texture. Further research is warranted to optimize the key synthesis parameters: PVA and graphite content, calcination temperature, and pressing pressure.

Acknowledgement

The authors would like to acknowledge the financial supports from the University of Sistan and Baluchestan, Islamic Republic of Iran.

Declaration of interest statement

The authors declare that they have no conflict of interest.

References

[1] Ordóñez C, Martínez I, Murillo R. Nickel catalyst supported on mayenite/CaO for the catalytic steam reforming of a tar model compound. Appl Catal A Gen. 2025;700:12026.

[2] Rong Q, Zhang X, Yan L, Wang S, Liu N, Zhou S, et al. Preparation and thermal emission properties of LaB6 enhanced nanocomposite C12A7 electrides-based composites. Ceram Int. 2025;51(7):8269-76.

[3] Shuvarakova EI, Ilyina EV, Stoyanovskii VO, Veselov GB, Bedilo AF, Vedyagin AA. Exploration of optical, redox, and catalytic properties of vanadia-mayenite nanocomposites. J Compos Sci. 2022;6:308.

[4] Volodin AM, Kenzhin RM, Kapishnikov AV, Komarovskikh AY, Vedyagin AA. Aluminothermic synthesis of dispersed electrides based on mayenite: XRD and EPR study. Materials. 2022;15:8988.

[5] Kotschote NL, Ebbinghaus SG. Comparison of different reducing agents for the synthesis of mayenite electride C12A7:2e− and a new photometric method to determine its electron density. Mater Chem Phys. 2025;335:130513.

[6] Wang Z, Ge D, Wang J, Zhou X, Huang S. Electron structure engineering of mayenite via titanium induction for enhanced chloride capture and multi-pollutant scavenging. Colloids Surf A Physicochem Eng Asp. 2025;139435.

[7] Yang S, Kondo JN, Hayashi K, Hirano M, Domen K, Hosono H. Partial oxidation of methane to syngas over promoted C12A7. Appl Catal A Gen. 2004;277:239-46.
[8] Ilyina EV, Bedilo AF, Veselov GB, Gerus YY, Shuvarakova EI, Stoyanovskii VO, et al. Comparative study of Pd-mayenite catalysts prepared via aerogel approaches. Gels. 2022;8:809.
[9] Zhang X, Li Z, Xu M, Hosono H, Ye TN. Recent progress and prospects in active anion-bearing C12A7 mediated chemical reactions. J Mater Chem A. 2023.
[10] Ruszak M, Inger M, Witkowski S, Wilk M, Kotarba A, Sojka Z. Selective N2O removal from the process gas of nitric acid plants over ceramic 12CaO·7Al2O3 catalyst. Catal Lett. 2008;126:72-7.
[11] Intiso A, Martinez-Triguero J, Cucciniello R, Proto A, Palomares AE, Rossi F. A novel synthetic route to prepare high surface area mayenite catalyst for TCE oxidation. Catalysts. 2019;9:27.
[12] Fujita S, Suzuki K, Ohkawa M, Mori T, Iida Y, Miwa Y, et al. Oxidative destruction of hydrocarbons on a new zeolite-like crystal of Ca12Al10Si4O35 including O2− and O22− radicals. Chem Mater. 2003;15:255-63.
[13] Cucciniello R, Intiso A, Castiglione S, Genga A, Proto A, Rossi F. Total oxidation of trichloroethylene over mayenite (Ca12Al14O33) catalyst. Appl Catal B Environ. 2017;204:167-72.
[14] Jeevaratnam J, Glasser F, Glasser LD. Anion substitution and structure of 12CaO·7Al2O3. J Am Ceram Soc. 1964;47:105-6.
[15] Lacerda M, Irvine JTS, Glasser FP, West AR. High oxide ion conductivity in Ca12Al14O33. Nature. 1988;332:525-6.
[16] Chorkendorff I, Niemantsverdriet JW. Concepts of modern catalysis and kinetics. 3rd ed. Hoboken (NJ): John Wiley & Sons; 2017.
[17] Li C, Hirabayashi D, Suzuki K. Synthesis of higher surface area mayenite by hydrothermal method. Mater Res Bull. 2011;46:1307-10.
[18] Shuvarakova E, Bedilo A, Kenzhin R, Ilyina E, Gerus Y. Synthesis and investigation of finely dispersed calcium aluminates and catalysts based on them. Russ J Phys Chem B. 2022;16:411-20.
[19] Ude SN, Rawn CJ, Peascoe RA, Kirkham MJ, Jones GL, Payzant EA. High temperature X-ray studies of mayenite synthesized using the citrate sol-gel method. Ceram Int. 2014;40:1117-23.
[20] Rashad M, Mostafa A, Rayan D. Structural and optical properties of nanocrystalline mayenite Ca12Al14O33 powders synthesized using a novel route. J Mater Sci Mater Electron. 2016;27:2614-23.
[21] Meza-Trujillo I, Devred F, Gaigneaux EM. Production of high surface area mayenite (C12A7) via an assisted solution combustion synthesis toward catalytic soot oxidation. Mater Res Bull. 2019;119:110542.
[22] Matović B, Prekajski M, Pantić J, Bräuniger T, Rosić M, Zagorac D, et al. Synthesis and densification of single-phase mayenite (C12A7). J Eur Ceram Soc. 2016;36:4237-41.
[23] Qiao Y, Tian Y, Zhang J, Tang R, Che Y, Li J. Stepwise solidus synthesis method for a micro-mesoporous calcium aluminate catalyst. Patent. Google Patents; 2020.
[24] Ruszak M, Witkowski S, Pietrzyk P, Kotarba A, Sojka Z. The role of intermediate calcium aluminate phases in solid state synthesis of mayenite (Ca12Al14O33). Funct Mater Lett. 2011;4:183-6.
[25] Inoue Y, Kitano M, Kim SW, Yokoyama T, Hara M, Hosono H. Highly dispersed Ru on electride [Ca24Al28O64]4+(e−)4 as a catalyst for ammonia synthesis. ACS Catal. 2014;4:674-80.